台灣農業研究 (J. Taiwan Agric. Res.) 75(1):87–101 (2026)
https://doi.org/10.6156/JTAR.202603_75(1).0005

Research Article

Symptomatology of *Fusarium oxysporum* Causing Pitaya Fusarium Fruit Rot in Taiwan

Jun-Wei Fan[1], Jyh-Nong Tsai[2], and Chu-Ping Lin[3,*]

Abstract

Fan, J. W., J. N. Tsai, and C. P. Lin. 2026. Symptomatology of the *Fusarium oxysporum* causing pitaya Fusarium fruit rot in Taiwan. J. Taiwan Agric. Res. 75(1):87–101.

Fusarium fruit rot is one of the common postharvest diseases of pitaya fruit in Taiwan. Since 2013, infected postharvest fruits were collected, exhibiting symptoms such as light brown patches with transverse stripes, white mycelium on the surface, or water-soaked lesions in severe cases. Green spots and less frequently observed scarring or rot on the pedicels and junctional branches of young fruits were also collected. All isolates obtained from these tissues exhibited morphological characteristics like those of *Fusarium oxysporum*. Further examination of colony morphology and sporulation patterns, combined with multilocus phylogenetic analyses based on RNA polymerase II second largest subunit (*rpb2*) and translation elongation factor 1-α (*tef1*) confirmed that all isolates belonged to *F. oxysporum*. Through artificial inoculation, symptoms on the postharvest fruits caused by *F. oxysporum* were confirmed, with symptoms showing a strong correlation with environmental humidity. When inoculation was performed on the surface of field-growing young fruits, green spots appeared after the color transition stage. Interestingly, consistent with the observations in the field, these spots did not progress to typical Fusarium fruit rot as the fruit matured, suggesting that the green spot and fruit rot symptoms may arise from infections occurring at different stages of fruit development. Also, the symptom of scarring and rot on pedicels were confirmed by the inoculation on the growing young fruits. This is the first disease report of the diversified symptoms on pitaya fruits caused by *F. oxysporum*, which can be attributed to different environment conditions and inoculation stage.

Key words: Pitaya, Postharvest disease, Fusarium fruit rot, *Fusarium oxysporum*.

INTRODUCTION

The most popularly cultivated pitaya fruit (*Hylocereus* spp.) in Taiwan can mainly be categorized by the flesh into white-fleshed type (*H. undatus* Britt. & Rose) and red-fleshed type (*H. polyrhizus* Britt. & Rose and *H. costaricensis* Britt. & Rose) (Jiang & Yang 2015). It is one of the important economic fruit trees in Taiwan. According to the latest statistical data, in 2024, the cultivation area was approximately 2,576.5 ha, with a fruit production value reaching 2.79 billion NTD (Agricultural Statistics Data Inquiry, Ministry of Agriculture, https://agrstat.moa.gov.tw/sdweb/public/inquiry/InquireAdvance.aspx).

Various *Fusarium* species have been widely reported as pathogens of pitaya in Malaysia, Indonesia, Argentina, and other regions. These include *F. fujikuroi* Nirenberg, *F. proliferatum* (Matsushima) Nirenberg, *F. solani* (Mart.)

Received: June 5, 2025; Accepted: October 31, 2025.
* Corresponding author, e-mail: cplin@tari.gov.tw
[1] Project Assistant, Plant Pathology Division, Taiwan Agricultural Research Institute, Taichung City, Taiwan, ROC.
[2] Research Fellow and Division Director, Plant Pathology Division, Taiwan Agricultural Research Institute, Taichung City, Taiwan, ROC.
[3] Assistant Research Fellow, Plant Pathology Division, Taiwan Agricultural Research Institute, Taichung City, Taiwan, ROC.

Sacc., and *F. oxysporum* Schltdl., which cause symptoms such as stem rot and basal rot (Wright *et al*. 2007; Rita *et al*. 2013; Balendres & Bengoa 2019; Mohd *et al*. 2023). The study by Cui *et al*. (2011) identifies *F. oxysporum* to be the major pathogen responsible for postharvest fruit rot on imported pitaya in the market in China. In Taiwan, pitaya fruit diseases caused by *F. oxysporum* have been previously reported (Lin *et al*. 2014). Symptoms observed in diseased pitaya fruits included brown spots or postharvest rot with white mycelium. Moreover, *F. oxysporum* has also been isolated from mature fruits with green spots and from young fruits with rotted pedicels (Lin *et al*. 2023). However, previous reports have remained preliminary, without providing systematic scientific evidence to clarify the involvement of *F. oxysporum* in pitaya fruit rot or to comprehensively describe the diversity of its symptomatology.

In this study, diseased pitaya fruit samples were collected from various fields, and fungal isolates were obtained. The identities of these isolates were confirmed based on morphological and molecular characteristics. Furthermore, to comprehend the pathogenicity and symptom development of pathogens in both young and mature pitaya fruits, different inoculation conditions were tested to observe variations in symptoms.

MATERIALS AND METHODS

Fungal isolation and preservation

Survey locations included Waipu district, Taichung city; Erlin town, Changhua county; Mingjian township, and Jiji town, Nantou county; Erlun town, Yunlin county; Zhuqi township, Chiayi county; Dongshan district, Tainan county; Alian district, Kaohsiung city; Wandan township, Pingtung county; Sanxing township, Yilan county; and Yuli town, Hualien county.

Diseased fruits were collected and pathogen isolation were performed as followed: diseased tissues of approximately $4 \times 4 \times 1$ mm^3 were excised, soaked in 5% NaClO for surface sterilization for 20–30 s, dried of excess surface droplets with paper towels, and then placed on potato dextrose agar (PDA, Difco™, Franklin Lakes, NJ, USA) plates and incubated at room temperature (RT, 22–26℃) for 2–3 d. To further purified the isolates, a single conidium of each isolates was selected and transferred to a new PDA plate, which were then incubated at RT under a 12-h light cycle for 7–10 d. For long-term preservation, agar blocks (approximately $5 \times 5 \times 2$ mm^3) containing mycelia of isolates were excised and preserved in 100% sterile mineral oil (Sigma-Aldrich, Louis, MO, USA). Each isolate was maintained under its designated laboratory accession number, and detailed information is presented in Table 1.

Morphological observations

Representative isolates included F213214, obtained from fruit rot in Waipu District in 2013, and F220020, obtained in Alian District in 2020. These isolates were cultured on PDA plates and slants at 22–24℃ under continuous light for 7–10 d, and the colony morphology was observed. Microconidia were observed by culturing the isolates on PDA plates and slants under light at 22–24℃ for 3–7 d. Macroconidia were observed by culturing the isolates on PDA plates and slants for 3–14 d. Chlamydospores were observed by culturing the isolates on PDA slants for over 1 mo. For each spore type, the size of 50 randomly selected spores was measured. An Olympus BX40 microscope (Olympus, Tokyo, Japan) and Canon 50D camera (Canon, Tokyo, Japan) were used for the observations and photography.

Growth observations of isolates

The test isolates were cultured in the dark on PDA plates for 3–5 d. Fresh hyphal plugs were cut from the colony edges using a 0.6 cm agar punch and transferred to the edges of new PDA plates. To observe the optimum temperature for hypha growth of the isolates, these plates were incubated at temperatures ranging from 4 to 40℃ (in 4℃ intervals, totaling 10 temperatures). Each isolate was tested with 3 plates per temperature, providing 3 replicates. The growth rate of hyphae at different temperatures was measured. The linear growth distance was recorded daily. At

certain temperatures, the colonies covered the entire plate by day 10, so growth data from day 1–9 were measured. The daily growth rate for each plate was calculated as (growth distance at day 9 - growth distance at day 1) cm/8 d (unit: cm d^{-1}). The experiment was conducted 3 times, and the mean value was presented.

Molecular identification of pathogenic fungi

Extraction of fungal genomic DNA (gDNA)

For each isolate, mycelium was collected from PDA plates after incubation at 24℃ for 7–10 d. Genomic DNA was extracted using the Kaneka Easy DNA Extraction Kit version 2 (Funakoshi, Tokyo, Japan), and the extracted gDNA was stored at -20℃ for subsequent use.

Gene sequence amplification and sequencing

Genomic DNA extracted from the isolates was subjected to polymerase chain reaction (PCR) using specific primer pairs to amplify target sequences, including RNA polymerase II second largest subunit (*rpb2*) and translation elongation factor 1-α (*tef1*). The primer pairs used are listed in Table 2, and PCR conditions followed those described in the respective references with minor modifications.

After confirming the amplified products as single band via 1.5% agarose gel electrophoresis, they were sent to Tri-I Biotech Inc., Taiwan for

Table 1. List of the isolates which were isolated in this study and related information and accession numbers in GenBank.

Species	Isolates	Stages/symptoms	Year	Location	*rpb2*	*tef1*
F. oxysporum	F213124	postharvest/fruit rot	2013	Jiji	PP783793	PP731826
	F213214	postharvest/fruit rot	2013	Waipu	PP783794	PP731827
	F217077	young fruit/pedicel rot	2017	Erlin	PP783795	PP731828
	F217138	young fruit /green spot	2017	Erlin	PP783796	PP731829
	F217171	young fruit /green spot	2017	Erlun	PP783797	PP731830
	F218078	young fruit /pedicel rot	2018	Mingjian	PP783798	PP731831
	F218109	young fruit /pedicel rot	2018	Dongshan	PP783799	PP731832
	F219028	postharvest/fruit rot	2019	Waipu	PP783800	PP731833
	F213200	postharvest/fruit rot	2013	Zhuqi	PP783807	PP731840
	F219032	postharvest/fruit rot	2019	Alian	PP783808	PP731841
	F220020	postharvest/fruit rot	2020	Alian	PP783810	PP731843
	F221117	postharvest/fruit rot	2021	Alian	PP783811	PP731844
	F223034	postharvest/fruit rot	2023	Erlin	PP783812	PP731845
	F224057	young fruit/pedicel rot	2024	Mingjian	PV696124	PV696127
	F224071	young fruit/pedicel rot	2024	Erlin	PV696125	PV696128
	F224086	young fruit/pedicel rot	2024	Alian	PV696126	PV696129

Table 2. Primer pairs used for each gene region and polymerase chain reaction (PCR) conditions.

Gene/locus	Primer	Sequence (5'-3')	PCR amplification procedures	Reference
RNA polymerase II second largest subunit (*rpb2*)	5f2 7cr	GGGGWGAYCAGAAGAAGGC CCCATRGCTTGYTTRCCCAT	94℃: 90 s, (94℃: 30 s, 55℃: 90 s, 68℃: 2 min) × 40 cycles, 68℃: 5 min.	Liu *et al*. (1999); O'Donnell *et al*. (2007); Sung *et al*. (2007)
translation elongation factor 1-α (*tef1*)	EF1 EF2	ATGGGTAAGGARGACAAGAC GGARGTACCAGTSATCATGTT	95℃: 4 min, (94℃: 1 min, 55℃: 30s, 72℃: 90 s) × 35 cycles, 72℃: 10 min.	O'Donnell *et al*. (1998); Garmendia *et al*. (2018)

sequencing. If electrophoresis results showed multiple bands for the amplified products, the annealing temperature of PCR was increased to achieve a single, distinct amplification product before sequencing.

The raw sequences obtained from forward and reverse primers were assembled using Contig Express software (Vector NTI Advance 11.5, Invitrogen, Carlsbad, CA, USA), and unstable signal parts at both ends were trimmed to obtain the final sequencing result.

Phylogenetic analysis

The phylogenetic analysis was conducted using sequence data from 51 isolates, including 16 isolates in this study and 35 reference isolates obtained from the National Center for Biotechnology Information (NCBI) database. The reference isolates and outgroup were selected based on the closest matches obtained from Basic Local Alignment Search Tool (BLAST) searches using the sequences of the test isolates, and the general structure of *Fusarium* groups confirmed by published literature (Schroers *et al*. 2009; O'Donnell *et al*. 2012, 2013; Xia *et al*. 2019). Suitable isolate sequences were then retrieved from the NCBI database for comparison.

Sequences of the individual gene region were initially aligned using MAFFT Multiple Sequence Alignment Software Version 7 (Katoh & Standley 2013) with auto strategy. Gaps in both ends were deleted. These gene segments were subsequently used to construct two-gene (*rpb2* + *tef1*) concatenated phylogenetic trees. The phylogenetic tree was constructed using the maximum likelihood (ML) method. The optimal substitution model was predicted using MEGA X software (Kumar *et al*. 2018), with the model having the lowest Bayesian Information Criterion (BIC) value selected. The "use all sites" option was chosen for handling gaps and missing data.

The ML phylogenetic tree was constructed using MEGA X software, employing the heuristic Nearest-Neighbor-Interchange (NNI) method for tree searching. Branch support was tested with 1,000 bootstrap replicates.

Pathogenicity experiment

Test fruits of mature white-fleshed or red-fleshed pitaya were purchased from a farm in central Taiwan. Isolates F213214 and F220020 were chosen as test strains, cultured on PDA plates and incubated for 7–10 d under a 12-h photoperiod. Conidia were collected using sterile water, with microconidia comprising more than 95% of the spores. After filtering through sterilized gauze (8 layers), the spore concentration was adjusted to desired level for use as the inoculum. To fulfill Koch's postulates, mature fruits and field-growing fruits were independently inoculated, observed for the appearance of similar symptoms, and re-isolated to confirm the same pathogens.

Inoculation of mature fruits

Before inoculation, the fruits were surface-sterilized with 200 mg mL^{-1} NaClO for 1 min, then dried with paper towels. Each fruit was inoculated at 4 points, with or without wounded treatment. For wounding, a bundle of 10 insect pins (NO.3 DM0004-3; MegaView) was used to gently prick the fruit surface 15–20 times to a depth of about 1 mm. Sterile cotton, approximately 1 cm^3 in volume, was soaked in the spore suspension (1–5 × 10^6 spores mL^{-1}), stirred, and left to stand for over 3 min. During inoculation, the soaked cotton was picked up with tweezers, excess liquid was removed, and the cotton was placed on each inoculation point, secured with transparent tape. The inoculated fruits were then placed in a preservation box with a paper towel moistened with sterile water at the bottom to maintain relative humidity (RH) > 95%. The box was sealed and stored in a dark room at RT (24–28℃).

For the high and low humidity symptom comparison experiment, 10 μL of the spore suspension was dropped onto the inoculation point, followed by 10 μL of Bacto agar (Difco™, Franklin Lakes, NJ, USA). High humidity (avg. RH = 97.7% ± 3.3%) was maintained by sealing the preservation box lid, while low humidity (avg. RH = 78.7% ± 8.3%) was achieved by

partially covering the box. Temperature and humidity within the boxes were monitored using a temperature and RH data logger (MX2301, HOBO, Onset Computer Corporation, Bourne, MA, USA). The control group was treated with sterile water instead of the spore suspension. The experiment was conducted 3 times and showed similar results.

Inoculation of field-growing fruits

Beside the representative isolates, 2 additional isolates, F217077 and F218109, were included in the experiment. From June to September 2021, fruits at the initial fruiting stage (0 wk) from white-fleshed pitaya fruit plants grown at the field of Taiwan Agricultural Research Institute, Taichung City, Taiwan, ROC were selected for inoculation. The fruit surface or pedicel was pricked 10–15 times with insect pins. Sterile cotton soaked in a 2–3 × 10^6 mL^{-1} spore suspension was then squeezed with tweezers and fixed to the wound with transparent tape. The fruits were covered with kraft paper bags to minimize rainwater entry. Inoculations were performed weekly from the 0-wk stage until the fruits were about 2 wk old, just before color transition stage, with a total of 3 inoculations. New cotton was used for each inoculation. One wk after the third inoculation, the cotton was removed, and the fruits were rewrapped in kraft paper bags until maturity. The experiment was conducted 3 times and showed similar results.

After harvesting, the fruits were placed in plastic baskets with non-slip mats and paper towels at the bottom, with the addition of sterile water. The baskets were sealed with plastic wrap, with holes poked in the 4 corners for ventilation, and kept at RT for 1 wk for observation.

RESULTS

Symptom description of *F. oxysporum* on pitaya fruits

From 2013 to 2024, postharvest pitaya fruits exhibiting various disease symptoms were continuously collected across multiple regions in Taiwan. Observed symptoms on mature fruits of both white- and red-fleshed pitaya included light to dark brown spots with fine transverse stripes or white mycelium growth (Fig. 1A and B). In severe cases, water-soaked symptoms were also observed (Fig. 1B). Fungi showing morphological traits typical of *F. oxysporum* were repeatedly isolated from these symptomatic tissues. Notably, fungi with similar characteristics were also isolated from green spots on the fruit surfaces (Fig. 1C), with scabbed pedicels of young fruits, and rotting on the junctions of the branches (Fig. 1D–F). These symptomatic cases are widespread and commonly observed in commercial orchards throughout Taiwan. To distinguish it from rot caused by other pathogens, the fruit rot specifically caused by *Fusarium* species is referred to as "Fusarium fruit rot".

Morphological characteristics of *F. oxysporum* isolates

The morphology of representative isolates, F213214 and F220020, were examined. Isolates F213214 exhibits the following features: the front of the colony is white to pale vinaceous, while the reverse side is deeper reddish-purple (Fig. 2A and B). The colony edges are filiform with abundant and fluffy aerial mycelium. Microconidia are hyaline, ellipsoidal, with blunt ends, occasionally with 1 end slightly pointed, with 0–1 septa, measuring 4.0-(7.3)-11.0 μm (min.-avg.-max.) in length and 2.1-(2.5)-4.2 μm in width, with a length-to-width ratio of 1.3-(2.9)-5.5 (Table 3, Fig. 2C). Macroconidia are hyaline, long stick-shaped, with 2–4 septa, apical cells blunt to papillate, and basal cells foot-shaped, measuring 24.3-(43.0)-72.0 μm in length and 2.8-(4.5)-6.1 μm in width, resulting in a length-to-width ratio of 5.8-(9.6)-16.1 (Table 3, Fig. 2D). Chlamydospores are globose to subglobose, with a diam. of 5.4-(7.2)-8.9 μm (Table 3, Fig. 2E). The optimal growth temperature for the mycelium is 28℃, with growth nearly ceasing at 4℃ and no growth above 40℃. Isolate F220020 of *F. oxysporum* exhibited morphological characteristics similar to those of isolate F213214 (Fig. 2F–J). However, the macroconidia exhibited the typical hook-

shaped apical cells with 3–4 septa (Fig. 2I). The morphology of both representative isolates closely resembles the description of *F. oxysporum* in the literature (Leslie & Summerell 2006).

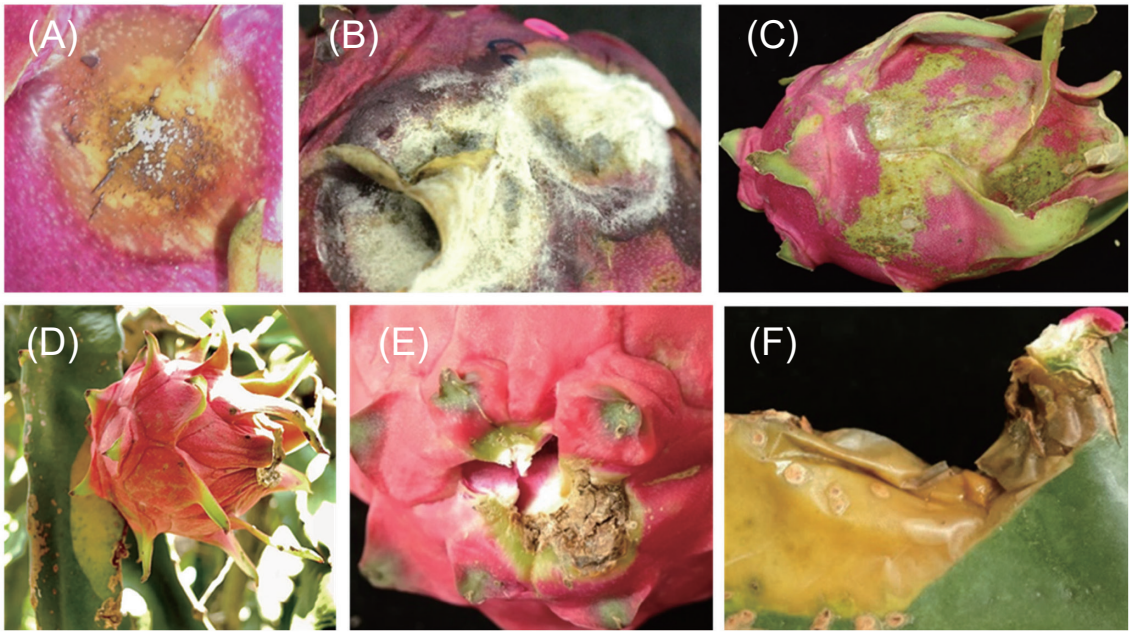

Fig. 1. The symptoms of pitaya Fusarium rot caused by *Fusarium oxysporum* in field, including (A, B) brown spots with transverse stripes or white mycelium on mature fruits, (C) green spots, and (D, E) scabbed pedicels of young fruits and (F) rotting on the junctional branch.

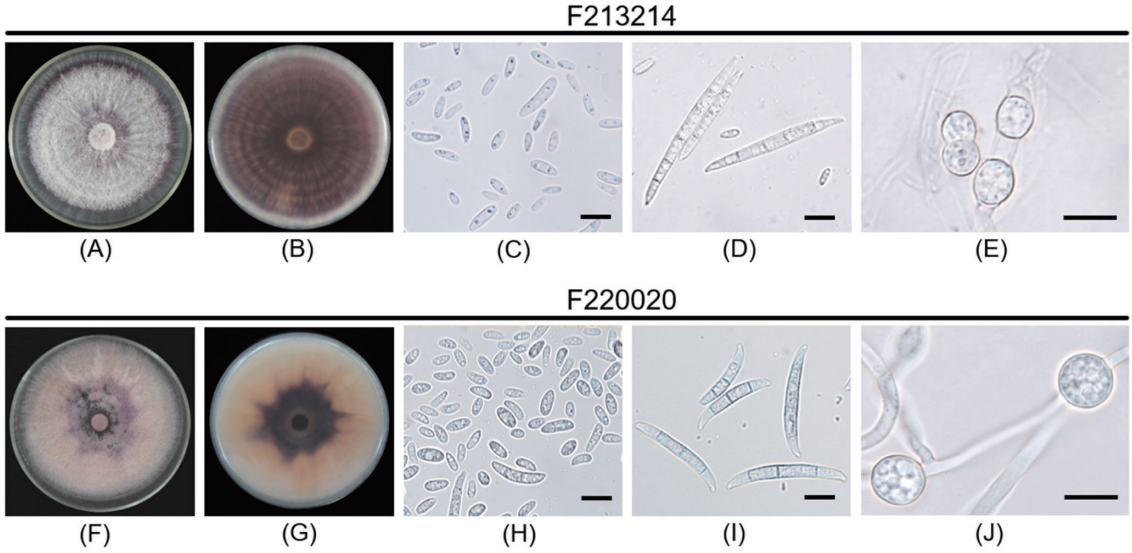

Fig. 2. Morphological features of the *Fusarium oxysporum* isolates F213214 and F220020. (A, F) Top and (B, G) reverse views of a colony. (C, H) Microconidia, (D, I) macroconidia, and (E, J) chlamydospore of each isolate were illustrated in one row from left to right. Bar = 10 μm.

Phylogenetic analysis of the *F. oxysporum* isolates

A ML phylogenetic tree was constructed using concatenated sequences of *rpb2* and *tef1* genes (Fig. 3). The analysis included 16 isolates from this study (Table 1), 30 *Fusarium* reference isolates, and 1 outgroup (*Cylindrocarpon cylindroides*), all obtained from published literature (Table 4). All 16 isolates in this study belonged to the *F. oxysporum* clade, supported by a 98% bootstrap value.

Both morphological and molecular identification results confirm that the two representative isolates belong to *F. oxysporum*.

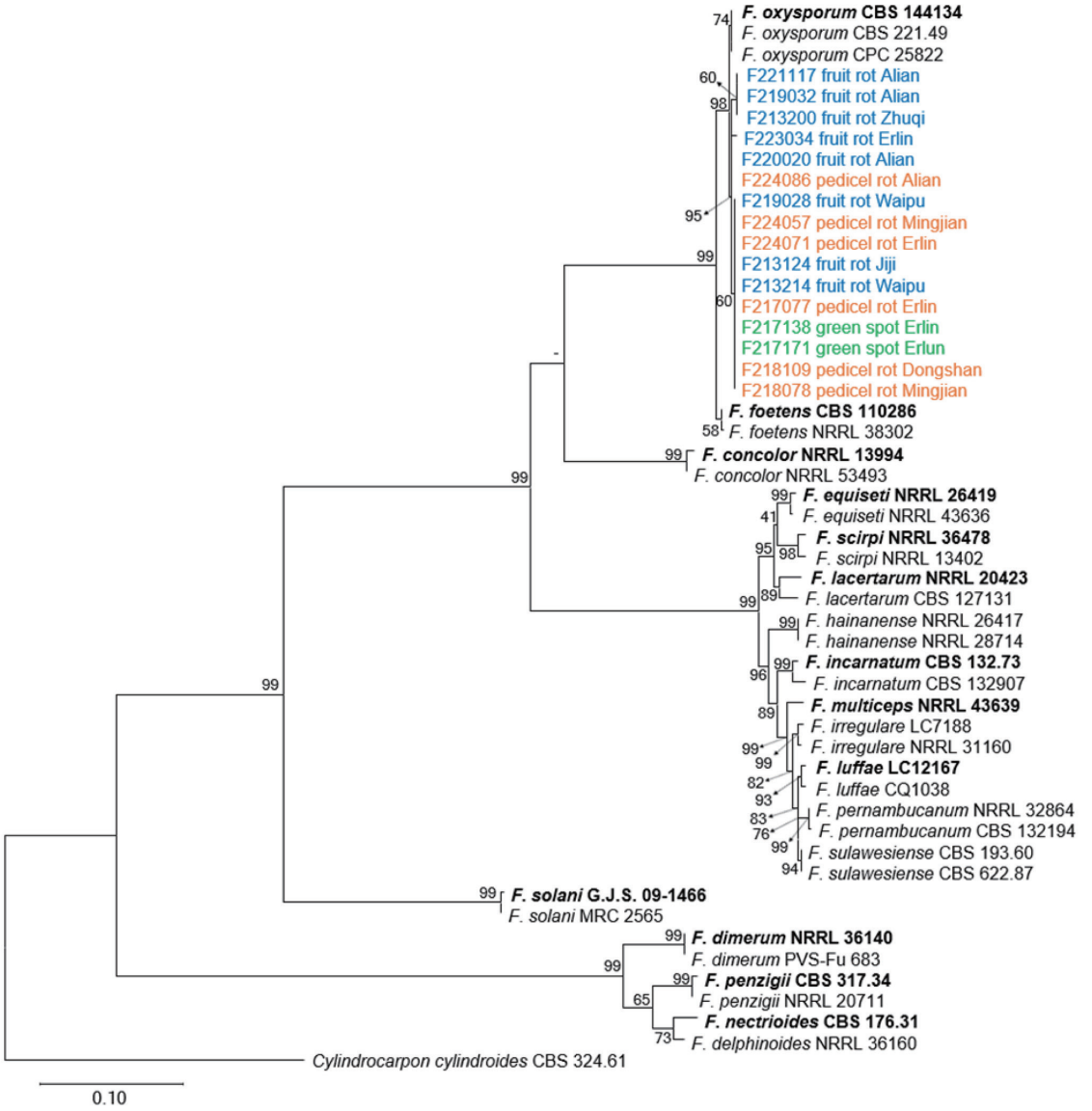

Fig. 3. Maximum likelihood (ML) phylogenetic tree based on RNA polymerase II second largest subunit (*rpb2*) and translation elongation factor 1-α (*tef1*) sequences of *Fusarium* spp. Isolates from this study are color-coded based on associated symptoms: blue for fruit rot, green for green spot, and orange for pedicel rot. Type strains are displayed in bold. Bootstrap support values (≥ 50%) are displayed at the nodes. The tree was rooted to *Cylindrocarpon cylindroides* CBS 324.61.

Table 3. Synopsis of morphological and physical data of the *Fusarium oxysporum* isolates in Taiwan.

Isolate no.	Microconidi length × width min.-avg.-max (μm), Length width ratio	Macroconidia length × width min.-avg.-max (μm), Length width ratio	Chlamydospore diameter min.-avg.-max (μm)	Optimum temperature for mycelium growth	Mycelium growth rate at optimum temperature (avg. ± *SE*, mm d^{-1})
F213214	4.0-(7.3)-11.0 × 2.1-(2.5)-4.2, 1.3-(2.9)-5.5	24.3-(43.0)-72.0 × 2.8-(4.5)-6.1, 5.8-(9.6)-16.1	5.4-(7.2)-8.9	28℃	5.6 ± 0.1
F220020	4.1-(6.6)-12.0 × 2.2-(2.8)-4.1, 1.3-(2.5)-4.5	24.1-(34.6)-49.1 × 3.2-(4.2)-6.0, 5.6-(8.4)-13.7	5.3-(8.9)-12.2	28℃	6.0 ± 0.0

Table 4. List of the reference isolates used in this study and related information and accession numbers.

Species	Isolates	*rpb2*	*tef1*	Reference
F. concolor	NRRL 13994^{T} = CBS 183.34	MH742569	MH742650	Crous *et al*. (2022)
	NRRL 53493	MH742614	MH742685	Jacobs-Venter *et al*. (2018)
F. delphinoides	NRRL 36160	HM347219	HM347134	O'Donnell *et al*. (2010)
F. dimerum	NRRL 36140^{T}	HM347218	HM347133	O'Donnell *et al*. (2010)
	PVS-Fu 683	MN540014	MT742267	Balmas *et al*. (2021)
F. equiseti	NRRL 26419^{T}	GQ505777	GQ505599	O'Donnell *et al*. (2009b)
	NRRL 43636	GQ505841	GQ505663	O'Donnell *et al*. (2009b)
F. foetens	CBS 110286^{T}	MT010984	MT011001	Brankovics *et al*. (2020)
	NRRL 38302	JX171652	FJ985444	O'Donnell *et al*. (2009a, 2013)
F. hainanense	NRRL 26417	GQ505776	GQ505598	O'Donnell *et al*. (2009b)
	NRRL 28714	GQ505782	GQ505604	O'Donnell *et al*. (2009b)
F. incarnatum	CBS 132.73^{T}	MN170409	MN170476	Xia *et al*. (2019)
	CBS 132907	MN170410	MN170477	Xia *et al*. (2019)
F. irregulare	LC7188	MK289783	MK289629	Wang *et al*. (2019)
	NRRL 31160	GQ505785	GQ505607	O'Donnell *et al*. (2009b)
F. lacertarum	CBS 127131	MN120739	MN120758	Lombard *et al*. (2019b)
	NRRL 20423^{T}	JX171581	GQ505593	Lombard *et al*. (2019b)
F. luffae	CQ1038	MK289723	MK289569	Wang *et al*. (2019)
	LC12167^{T}	MK289754	MK289601	Wang *et al*. (2019)
F. multiceps	NRRL 43639^{T}	GQ505844	GQ505666	O'Donnell *et al*. (2009b)
F. nectrioides	CBS 176.31^{T}	JX171591	EU926312	Schroers *et al*. (2009) O'Donnell *et al*. (2013)
F. oxysporum	CBS 144134^{T}	MH484953	MH485044	Lombard *et al*. (2019a)
	CBS 221.49	MH484872	MH484963	Lombard *et al*. (2019a)
	CPC 25822	MH484943	MH485034	Lombard *et al*. (2019a)
F. penzigii	CBS 317.34^{T}	KM232362	EU926324	Lombard *et al*. (2015)
	NRRL 20711	HM347217	HM347132	O'Donnell *et al*. (2010)
F. pernambucanum	CBS 132194	MN170425	MN170492	Xia *et al*. (2019)
	NRRL 32864	GQ505791	GQ505613	O'Donnell *et al*. (2009b)
F. scirpi	NRRL 13402	JX171566	GQ505592	Sandoval-Denis *et al*. (2018)
	NRRL 36478^{T}	GQ505832	GQ505654	O'Donnell *et al*. (2009b)

Table 4. List of the reference isolates used in this study and related information and accession numbers. (continued)

Species	Isolates	*rpb2*	*tef1*	Reference
F. solani	G.J.S. 09-1466[T]	KT313623	KT313611	Schroers *et al*. (2016)
	MRC 2565	MH582410	MH582420	O'Donnell *et al*. (2018)
F. sulawesiense	CBS 193.60	MN170435	MN170502	Xia *et al*. (2019)
	CBS 622.87	MN170436	MN170503	Xia *et al*. (2019)
outgroup *Cylindrocarpon cylindroides*	CBS 324.61	DQ789803	JF735788	Castlebury *et al*. (2006)

[T] Type strains.

Pathogenicity of *F. oxysporum* on mature fruits

Pathogenicity experiments were conducted on mature white-fleshed pitaya fruits. The results showed similar symptoms for both representative isolates. Under high humidity, brown water-soaked lesions appeared at the inoculation points 3–5 d after inoculation at RT and RH > 95%, accompanied by white fungal colony growth, and the same pathogens were re-isolated (Fig. 4A, B). Similar results were observed when the same isolates were tested on the red-fleshed pitaya fruits (Fig. 4C and D). Symptoms developed in both wounded and unwounded treatments, but progressed more rapidly in the wounded fruits (data not shown).

To confirm the effect of humidity on symptom development, inoculated fruits were placed under relatively low RH instead of high RH conditions. Under relatively low RH, both representative isolates caused similar symptoms: light brown spots, without water-soaking, appeared at the inoculation points 3–5 d after inoculation (Fig. 4E and F).

These symptoms described above resembled those commonly observed under field conditions. The same pathogens could be re-isolated from the symptomatic tissues, thereby fulfilling Koch's postulates. In the control group, some inoculation sites developed brown scabs indicative of physiological wounds (data not shown), which were distinct from symptoms caused by *F. oxysporum*, and no suspected pathogens were re-isolated from these sites.

Green spots and pedicel rot caused by *F. oxysporum*

To confirm the relationship between green spot symptoms and *F. oxysporum*, spore suspensions of the F213214 and F220020 isolates were individually inoculated on the surface of 0-wk-old white-fleshed pitaya fruits in the field. The symptoms were monitored continuously until the fruits changed color, matured, and then were harvested. After the fruits changed color, green spot symptoms appeared at the inoculation points with both isolates (Fig. 5A and B). However, after mature fruit harvesting, when the inoculated fruits were placed in a RT and high humidity environment, the green spots did not expand, nor did they develop into typical symptoms such as blocky brown spots or water-soaked rot caused by *F. oxysporum*. So did the natural infected samples with green spots.

To confirm the symptoms of scabbed pedicels and rotting on junctional branches caused by *F. oxysporum*, both representative isolates were tested by inoculating the pedicels of young fruits of white-fleshed pitaya. Inoculation with the *F. oxysporum* representative isolate F213214 resulted only in green spots (Fig. 5C). Additional isolates of *F. oxysporum*, F217077 and F218109, exhibited similar responses as the F213214 isolate (data not shown). However, inoculation with the other representative isolate F220020 caused infection symptoms at the junctions of pedicels and branches (Fig. 5D and E), similar to those observed in field pedicel tissues.

The same pathogens were re-isolated from all the symptomatic tissues, confirming their

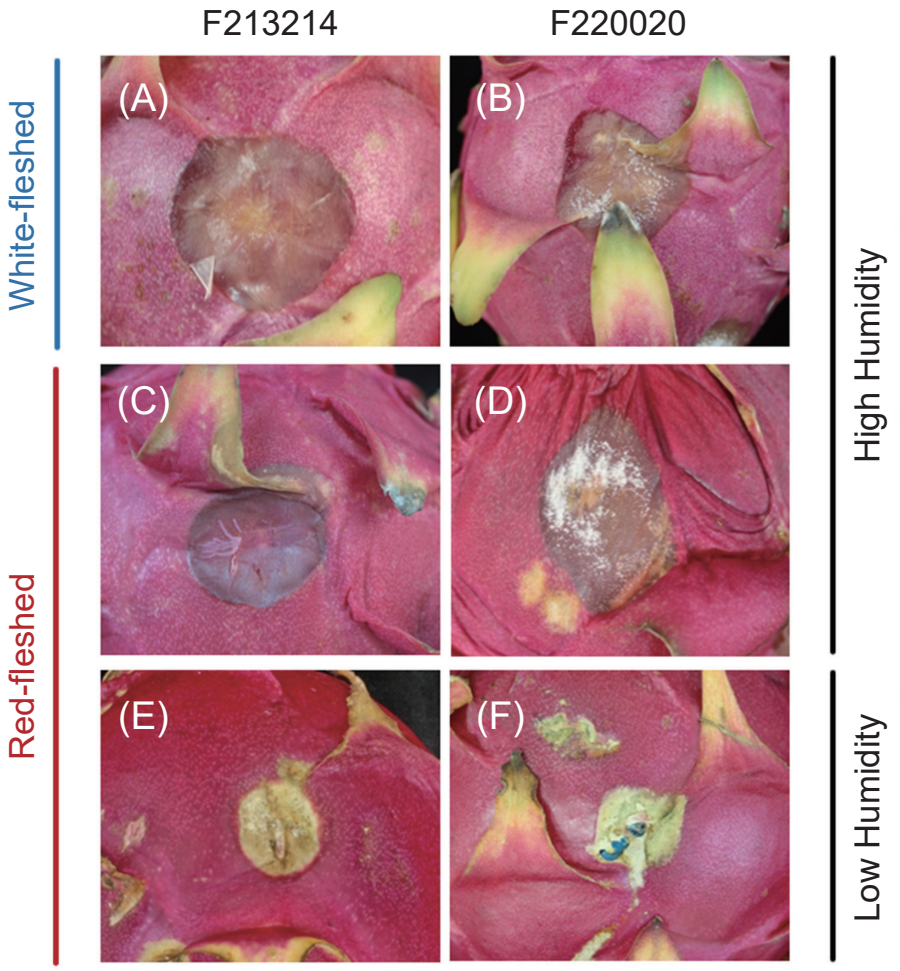

Fig. 4. Symptoms of artificial inoculation mature pitaya fruits, with test strains F213214 and F220020 (*Fusarium oxysporum*). (A, B) on white-fleshed fruits; (C–F) on red-fleshed fruits.

pathogenicity and thus, fulfilling the Koch's postulates. The control group showed no significant symptoms, and no suspected pathogens were isolated.

DISCUSSION

Based on the morphological, sequence analyses, and pathogenicity test, it is confirmed that *F. oxysporum* can induce a diverse range of symptoms on pitaya (Fig. 1). Postharvest fruits exhibit both dry brown spot symptoms and water-soaked lesions, with a strong correlation to humidity (Fig. 4); whereas young fruits may develop green spots, pedicel scabs, and rot at the junctional branches.

Intriguingly, through artificial inoculation experiments, it was revealed that postharvest symptoms only appeared in experiments where mature fruits were directly inoculated with *F. oxysporum*. No fruit rot symptoms occurred after harvest when inoculated on immature fruits before color transition stage (Fig. 5). From this, it can be deduced that the timing of infection for Fusarium fruit rot, which occurs after harvest, is close to maturity of fruits.

The same fungal isolates were re-isolated from the green spot symptoms, indicating the

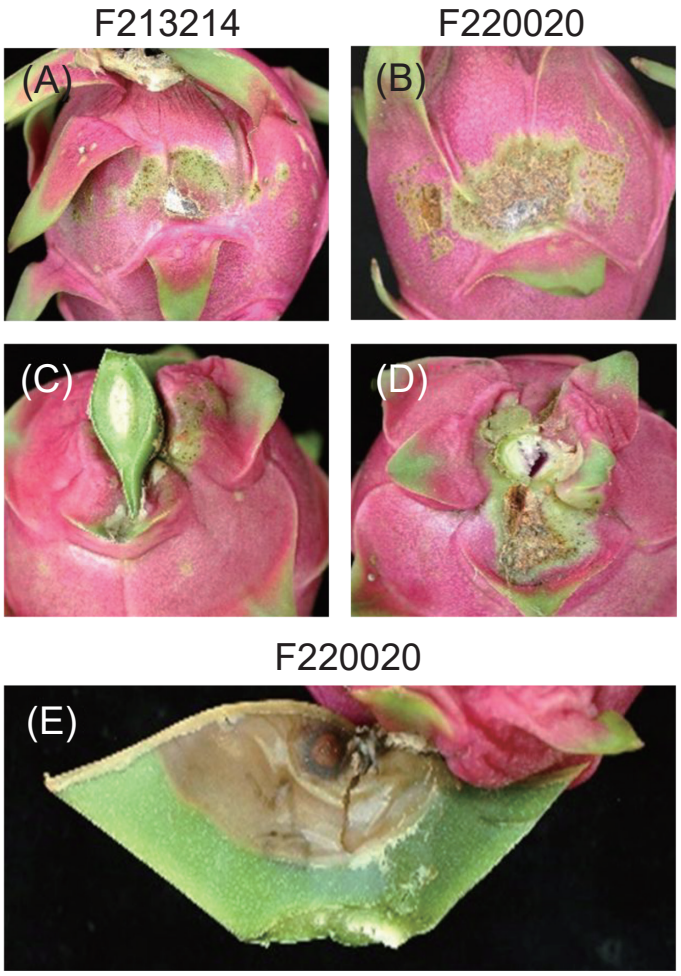

Fig. 5. Symptoms of artificial inoculation on young pitaya fruits in the fields, with strains F213214 and F220020 (*Fusarium oxysporum*). (A, B) inoculated on fruit surface; (C–E) inoculated at the junction of pedicel and branch.

persistence of the pathogen at the inoculation sites even after fruit maturation. Pitaya fruits are green during their immature stage, gradually turning red during maturation due to factors such as chlorophyll degradation and anthocyanin accumulation during the late developmental stage (Wybraniec *et al*. 2007; Phebe *et al*. 2009). Additionally, young fruits contain higher levels of phenolic compounds compared to mature fruits (Singh *et al*. 2022). Phenolic compounds are not only related to plant physiology but are also highly correlated with the ability to resist pathogen invasion (Pratyusha 2022). It is speculated that when young fruits are infected by *F. oxysporum*, they trigger specific defense mechanisms such as maintaining higher levels of phenolic compounds (Kumar *et al*. 2020) or other secondary metabolites with antimicrobial properties (Zaynab *et al*. 2018), accumulating high amounts of callose (Luna *et al*. 2011), altering tissue structure, or producing papillae to form barriers (Underwood 2012). These responses may confine the pathogen to the infection sites, preventing further fruit rot, but causing abnormal pigment metabolism that results in green spot formation.

In field surveys, *F. oxysporum* was found to cause pedicel scabs or rot at the junctional

branches occasionally. In artificial inoculation experiments, only 1 of the 4 isolates used in the tests could cause similar symptoms and fulfill the Koch's postulates. The conditions for pedicel and branch rot caused by *F. oxysporum* in the field require further study.

Comprehensive field investigations are needed to clarify these findings and to better understand the ecological dynamics of *F. oxysporum* in pitaya cultivation. The potential sources of infection remain uncertain. Although *F. oxysporum* is typically regarded as a soilborne pathogen (Joshi 2018; Srinivas *et al*. 2019), the occurrence of symptoms on aerial fruit tissues in this study suggests alternative modes of dissemination. One possibility is that wind and rain splash soilborne propagules onto the fruits; another is that small insects or snails may contribute to pathogen dispersal. Further studies are warranted to test these hypotheses. Interestingly, there have been report of stem rot in pitaya caused by *F. oxysporum* infection in Taiwan (Tsai 2004). However, *F. oxysporum* exhibits host-specific specialization through its *formae speciales*, and the pathogenicity among different isolates or *formae speciales* is highly variable. Moreover, several studies have considered *F. oxysporum* as a species complex (Laurence *et al*. 2014; Brankovics *et al*. 2020; Panno *et al*. 2021). Further studies are required to determine whether *F. oxysporum* isolates responsible for stem rot can also cause symptoms in aerial parts of pitaya, such as pedicel scabs, branch rot at the junctions, and fruit rot.

In conclusion, this study systematically confirms that *F. oxysporum* is the primary causal agent of pitaya fruit rot in Taiwan and is responsible for a wide spectrum of symptoms. The variation in symptom expression may be influenced by environmental humidity and the timing of infection. However, the conditions under which *F. oxysporum* causes pedicel rot remain to be studied. Additionally, the ecology of *F. oxysporum* needs to be further investigated to efficiently prevent the occurrence of Fusarium fruit rot.

ACKNOWLEDGMENTS

This article was supported by funding from the Taiwan Agricultural Research Institute, Ministry of Agriculture under projects 112 Agricultural Science-5.3.1-Agriculture-C1(4) and 113 Agricultural Science-5.3.1-Agriculture-01(3). Assistant Er-Xuan, Li aided in the investigation and experimentation process.

REFERENCES

Balendres, M. A. and J. C. Bengoa. 2019. Diseases of dragon fruit (*Hylocereus* species): Etiology and current management options. Crop Prot. 126:104920. doi:10.1016/j.cropro.2019.104920

Balmas, V., F. Fancellu, S. Sanna, B. Scherm, Q. Migheli, and I. Malbrán. 2021. Water distribution systems in Sardinian hospitals host invasive clonal lineages of the *Fusarium oxysporum* and *Fusarium solani* species complexes. Mycologia 113:725–733. doi:10.1080/00275514.2021.1905497

Brankovics, B., A. D. van Diepeningen, G. S. de Hoog, T. A. J. van der Lee, and C. Waalwijk. 2020. Detecting introgression between members of the *Fusarium fujikuroi* and *F. oxysporum* species complexes by comparative mitogenomics. Front. Microbiol. 11:1092. doi:10.3389/fmicb.2020.01092

Castlebury, L. A., A. Y. Rossman, and A. S. Hyten. 2006. Phylogenetic relationships of *Neonectria/Cylindrocarpon* on *Fagus* in North America. Botany 84:1417–1433. doi:10.1139/b06-105

Crous, P. W., M. Sandoval-Denis, M. M. Costa, J. Z. Groenewald, A. L. van Iperen, M. Starink-Willemse, ... M. Thines. 2022. *Fusarium* and allied fusarioid taxa (FUSA). 1. Fungal Syst. Evol. 9:161–200. doi:10.3114/fuse.2022.09.08

Cui, Z. J., Y. W. Wang, Y. Yu, and L. Xu. 2011. Pathogens analysis of soft rot disease of imported pitaya in Shanghai. Microbiol. China 38:1499–1506. (in Chinese)

Garmendia, G., M. Umpierrez-Failache, T. J. Ward, and S. Vero. 2018. Development of a PCR-RFLP method based on the transcription elongation factor 1-α gene to differentiate *Fusarium graminearum* from other species within the *Fusarium graminearum* species complex. Food Microbiol. 70:28–32. doi:10.1016/j.fm.2017.08.020

Jacobs-Venter, A., I. Laraba, D. M. Geiser, M. Busman, M. M. Vaughan, R. H. Proctor, … K. O'Donnell. 2018. Molecular systematics of two sister clades, the *Fusarium concolor* and *F. babinda* species

complexes, and the discovery of a novel microcycle macroconidium- Producing species from South Africa. Mycologia 110:1189–1204. doi:10.1080/00275514.2018.1526619

Joshi, R. 2018. A review of *Fusarium oxysporum* on its plant interaction and industrial use. J. Med. Plants Stud. 6(3):112–115. doi:10.22271/plants.2018.v6.i3b.07

Jiang, Y. L. and W. J. Yang. 2015. The effects of heavy shading and flowering thinning in summer on off-season production in red pitaya (*Hylocereus* sp.). J. Taiwan Soc. Hort. Sci. 61:69–77. (in Chinese with English abstract) doi:10.6964/JTSHS.201506_61(2).0001

Katoh, K. and D. M. Standley. 2013. MAFFT multiple sequence alignment software version 7: Improvements in performance and usability. Mol. Biol. Evol. 30:772–780. doi:10.1093/molbev/mst010

Kumar, S., M. M. Abedin, A. K. Singh, and S. Das. 2020. Role of phenolic compounds in plant-defensive mechanisms. p.517–532. *in*: Plant Phenolics in Sustainable Agriculture. (Lone, R., R. Shuab, and A. N. Kamili, eds.) Springer. Singapore. 594 pp. doi:10.1007/978-981-15-4890-1_22

Kumar, S., G. Stecher, M. Li, C. Knyaz, and K. Tamura. 2018. MEGA X: Molecular evolutionary genetics analysis across computing platforms. Mol. Biol. Evol. 35:1547–1549. doi:10.1093/molbev/msy096

Laurence, M. H., B. A. Summerell, L. W. Burgess, and E. C. Liew. 2014. Genealogical concordance phylogenetic species recognition in the *Fusarium oxysporum* species complex. Fungal Biol. 118:374–384. doi:10.1016/j.funbio.2014.02.002

Leslie, J. F. and B. A. Summerell 2006. The *Fusarium* Laboratory Manual. Blackwell Publishing. Ames, IA. 388 pp. doi:10.1002/9780470278376

Lin, C. P., J. N. Tsai, P. J. Ann, T. H. Hsu, J. T. Chang, and T. Y. Kuo. 2014. Survey and study of postharvest diseases of dragon fruits in Taiwan. Taiwan Phytopathol. Soc. 23:174–235. (Abstract in Chinese)

Lin, C. P., J. N. Tsai, P. J. Ann, and E. S. Li. 2023. Pitaya fruit rot caused by *Fusarium oxysporum* species complex. Meet. J. Plant Med. 65:178–179. (Abstract in Chinese)

Liu, Y. J., S. Whelen, and B. D. Hall. 1999. Phylogenetic relationships among ascomycetes: Evidence from an RNA polymerse II subunit. Mol. Biol. Evol. 16:1799–1808. doi:10.1093/oxfordjournals.molbev.a026092

Lombard, L., M. Sandoval-Denis, S. C. Lamprecht, and P. W. Crous. 2019a. Epitypification of *Fusarium oxysporum*- Clearing the taxonomic chaos. Persoonia 43:1–47. doi:10.3767/persoonia.2019.43.01

Lombard, L., N. A. van der Merwe, J. Z. Groenewald, and P. W. Crous. 2015. Generic concepts in *Nectriaceae*. Stud. Mycol. 80:189–245. doi:10.1016/j.simyco.2014.12.002

Lombard, L., R. Van Doorn, and P. W. Crous. 2019b. Neotypification of *Fusarium chlamydosporum*- A reappraisal of a clinically important species complex. Fungal Syst. Evol. 4:183–200. doi:10.3114/fuse.2019.04.10

Luna, E., V. Pastor, J. Robert, V. Flors, B. Mauch-Mani, and J. Ton. 2011. Callose deposition: A multifaceted plant defense response. Mol. Plant Microbe Interact. 24:183–193. doi:10.1094/MPMI-07-10-0149

Mohd, M. H., N. M. I. M. Nor, N. F. Azuddin, and L. Zakaria. 2023. Mycotoxin production by *Fusarium proliferatum* and *Fusarium fujikuroi* causing stem rot of *Hylocereus polyrhizus* in Malaysia. Malays. Appl. Biol. 52(3):13–22. doi:10.55230/mabjournal.v52i3.2644

O'Donnell, K., C. Gueidan, S. Sink, P. R. Johnston, P. W. Crous, A. Glenn, … B. A. J. Sarver. 2009a. A two-locus DNA sequence database for typing plant and human pathogens within the *Fusarium oxysporum* species complex. Fungal Genet. Biol. 46:936–948. doi:10.1016/j.fgb.2009.08.006

O'Donnell, K., R. A. Humber, D. M. Geiser, S. Kang, B. Park, V. A. R. G. Robert, … S. A. Rehner. 2012. Phylogenetic diversity of insecticolous fusaria inferred from multilocus DNA sequence data and their molecular identification via FUSARIUM-ID and *Fusarium* MLST. Mycologia 104:427–445. doi:10.3852/11-179

O'Donnell, K., H. C. Kistler, E. Cigelnik, and R. C. Ploetz. 1998. Multiple evolutionary origins of the fungus causing Panama disease of banana: Concordant evidence from nuclear and mitochondrial gene genealogies. Proc. Natl. Acad. Sci. U.S.A. 95:2044–2049. doi:10.1073/pnas.95.5.2044

O'Donnell, K., S. P. McCormick, M. Busman, R. H. Proctor, T. J. Ward, G. Doehring, … J. P. Rheeder. 2018. Marasas *et al*. 1984 "Toxigenic *Fusarium* species: Identity and mycotoxicology" revisited. Mycologia 110:1058–1080. doi:10.1080/00275514.2018.1519773

O'Donnell, K., A. P. Rooney, R. H. Proctor, D. W. Brown, S. P. McCormick, T. J. Ward, … D. M. Geiser. 2013. Phylogenetic analyses of *RPB1* and *RPB2* support a middle Cretaceous origin for a clade comprising all agriculturally and medically important fusaria. Fungal Genet. Biol. 52:20–31. doi:10.1016/j.fgb.2012.12.004

O'Donnell, K., B. A. J. Sarver, M. Brandt, D. C. Chang, J. Noble-Wang, B. J. Park, ... T. J. Ward. 2007.

Phylogenetic diversity and microsphere array-based genotyping of human pathogenic fusaria, including isolates from the multistate contact lens-associated U.S. keratitis outbreaks of 2005 and 2006. J. Clin. Microbiol. 45:2235–2248. doi:10.1128/jcm.00533-07

O'Donnell, K., D. A. Sutton, M. G. Rinaldi, C. Gueidan, P. W. Crous, and D. M. Geiser. 2009b. Novel multilocus sequence typing scheme reveals high genetic diversity of human pathogenic members of the *Fusarium incarnatum-F*. equiseti and *F. chlamydosporum* species complexes within the United States. J. Clin. Microbiol. 47:3851–3861. doi:10.1128/jcm.01616-09

O'Donnell, K., D. A. Sutton, M. G. Rinaldi, B. A. J. Sarver, S. A. Balajee, H. J. Schroers, ... D. M. Geiser. 2010. Internet-accessible DNA sequence database for identifying fusaria from human and animal infections. J. Clin. Microbiol. 48:3708–3718. doi:10.1128/JCM.00989-10

Panno, S., S. Davino, A. G. Caruso, S. Bertacca, A. Crnogorac, A. Mandić, ... S. Matić. 2021. A review of the most common and economically important diseases that undermine the cultivation of tomato crop in the mediterranean basin. Agronomy 11:2188. doi:10.3390/agronomy11112188

Phebe, D., M. K. Chew, A. A. Suraini, O. M. Lai, and O. A. Janna. 2009. Red-fleshed pitaya (*Hylocereus polyrhizus*) fruit colour and betacyanin content depend on maturity. Intl. Food Res. J. 16:233–242.

Pratyusha, S. 2022. Phenolic compounds in the plant development and defense: An overview. p.125–140. *in*: Plant Stress Physiology-Perspectives in Agriculture. (Hasanuzzaman, M. and K. Nahar, eds.) IntechOpen. London, UK. 224 pp. doi:10.5772/intechopen.102873

Rita, W. S., D. N. Suprapta, I. M. Sudana, and I. M. D. Swantara. 2013. First report on *Fusarium solani*, a pathogenic fungus causing stem rot disease on dragon fruits (*Hylocereus* sp.) in Bali. J. Biol. Agric. Healthc. 3(17):93–99.

Sandoval-Denis, M., V. Guarnaccia, G. Polizzi, and P. W. Crous. 2018. Symptomatic Citrus trees reveal a new pathogenic lineage in *Fusarium* and two new *Neocosmospora* species. Persoonia 40:1–25. doi:10.3767/persoonia.2018.40.01

Schroers, H. J., K. O'Donnell, S. C. Lamprecht, P. L. Kammeyer, S. Johnson, D. A. Sutton, ... R. C. Summerbell. 2009. Taxonomy and phylogeny of the *Fusarium dimerum* species group. Mycologia 101:44–70. doi:10.3852/08-002

Schroers, H. J., G. J. Samuels, N. Zhang, D. P. G. Short, J. Juba, and D. M. Geiser. 2016. Epitypification of *Fusisporium* (*Fusarium*) *solani* and its assignment to a common phylogenetic species in the *Fusarium solani* species complex. Mycologia 108:806–819. doi:10.3852/15-255

Singh, A., S. Swami, N. R. Panwar, M. Kumar, A. K. Shukla, Y. Rouphael, ... P. Kumar. 2022. Development changes in the physicochemical composition and mineral profile of red-fleshed dragon fruit grown under semi-arid conditions. Agronomy 12:355. doi:10.3390/agronomy12020355

Srinivas, C., D. N. Devi, K. N. Murthy, C. D. Mohan, T. R. Lakshmeesha, B. Singh, ... R. K. Srivastava. 2019. *Fusarium oxysporum* f. sp. *lycopersici* causal agent of vascular wilt disease of tomato: Biology to diversity- A review. Saudi J. Biol. Sci. 26:1315–1324. doi:10.1016/j.sjbs.2019.06.002

Sung, G. H., J. M. Sung, N. L. Hywel-Jones, and J. W. Spatafora. 2007. A multi-gene phylogeny of Clavicipitaceae (Ascomycota, Fungi): Identification of localized incongruence using a combinational bootstrap approach. Mol. Phylogenet. Evol. 44:1204–1223. doi:10.1016/j.ympev.2007.03.011

Tsai, Y. F. 2004. Investigation on the cause of stem rot disease in dragon fruit. Master Thesis. Department of Plant Protection, National Pingtung University of Science and Technology. Pingtung, Taiwan. 276 pp. (in Chinese with English abstract)

Underwood, W. 2012. The plant cell wall: A dynamic barrier against pathogen invasion. Front. Plant Sci. 3:85. doi:10.3389/fpls.2012.00085

Wang, M. M., Q. Chen, Y. Z. Diao, W. J. Duan, and L. Cai. 2019. *Fusarium incarnatum-equiseti* complex from China. Persoonia 43:70–89. doi:10.3767/persoonia.2019.43.03

Wright, E. R., M. C. Rivera, A. Ghirlanda, and G. A. Lori. 2007. Basal rot of *Hylocereus undatus* caused by *Fusarium oxysporum* in Buenos Aires, Argentina. Plant Dis. 91:323. doi:10.1094/PDIS-91-3-0323A

Wybraniec, S., B. Nowak-Wydra, K. Mitka, P. Kowalski, and Y. Mizrahi. 2007. Minor betalains in fruits of *Hylocereus* species. Phytochemistry 68:251–259. doi:10.1016/j.phytochem.2006.10.002

Xia, J. W., M. Sandoval-Denis, P. W. Crous, X. G. Zhang, and L. Lombard. 2019. Numbers to names-Restyling the *Fusarium incarnatum-equiseti* species complex. Persoonia 43:186–221. doi:10.3767/persoonia.2019.43.05

Zaynab, M., M. Fatima, S. Abbas, Y. Sharif, M. Umair, M. H. Zafar, and K. Bahadar. 2018. Role of secondary metabolites in plant defense against pathogens. Microb. Pathog. 124:198–202. doi:10.1016/j.micpath.2018.08.034

引起臺灣紅龍果鐮孢果腐病 *Fusarium oxysporum* 之病徵探討

范浚維[1] 蔡志濃[2] 林筑蘋[3,*]

摘要

范浚維、蔡志濃、林筑蘋。2026。引起臺灣紅龍果鐮孢果腐病 *Fusarium oxysporum* 之病徵探討。台灣農業研究 75(1):87–101。

鐮孢果腐病 (Fusarium fruit rot) 為臺灣紅龍果常見的採收後果實病害之一。自 2013 年起，採集罹染鐮孢果腐病的採收後果實，包含果表帶有橫紋或白色菌絲之塊狀褐斑，嚴重者呈水浸狀腐爛；或田間果實表面綠斑、幼果果梗處結痂及連接處腐爛等病徵。病徵經過組織分離後皆可得與 *Fusarium oxysporum* 形態特徵相似的分離株。進一步觀察菌落與產孢形態，以及利用 RNA polymerase II second largest subunit (*rpb2*) 與 translation elongation factor 1-α (*tef1*) 等 2 序列片段做多重序列親緣關係分析，確認皆屬 *F. oxysporum*。透過人工接種採收後果實，確認 *F. oxysporum* 引起之採後果實病徵，且病徵表現與環境濕度關係性高；接種於田間幼果表面時，接種點於果實轉色期後呈現綠斑，有趣的是，與田間發現的綠斑果實狀況一致，後續果實成熟後不會進展為鐮孢果腐病。亦透過接種田間幼果果梗確認 *F. oxysporum* 菌株可引起結痂或腐爛。本研究為首篇確認 *F. oxysporum* 可引起紅龍果果實多型病徵之報導，並確認其病徵差異與環境條件以及接種時機有關。

關鍵詞：紅龍果、採後病害、鐮孢果腐病、*Fusarium oxysporum*。

投稿日期：2025 年 6 月 5 日；接受日期：2025 年 10 月 31 日。
* 通訊作者：cplin@tari.gov.tw
[1] 農業部農業試驗所植物病理組計畫助理。臺灣 臺中市
[2] 農業部農業試驗所植物病理組研究員兼組長。臺灣 臺中市。
[3] 農業部農業試驗所植物病理組助理研究員。臺灣 臺中市。